

Antisense Imaging: And Miles to go Before we Sleep?

Michael R. Lewis^{1,2,3*} and Fang Jia¹

¹Department of Veterinary Medicine and Surgery, University of Missouri-Columbia, Columbia, Missouri 65211

²Department of Radiology, University of Missouri-Columbia, Columbia, Missouri 65211

³Nuclear Science and Engineering Institute, University of Missouri-Columbia, Columbia, Missouri 65211

Abstract Labeled oligonucleotide analogues for antisense imaging of messenger RNA (mRNA) have great potential for detection of endogenous gene expression in vivo. Successful antisense imaging may be useful for detecting cellular gene expression patterns and early molecular changes in disease. Conclusive demonstration of this technique has been hindered by formidable challenges in surmounting biological barriers and detecting low concentrations of target mRNA. Recent advances in the development of novel antisense molecules, high specific activity radiolabeling chemistry, sophisticated drug targeting technology, and complementary molecular imaging modalities make it quite possible that true antisense imaging will be realized in the near future. *J. Cell. Biochem.* 90: 464–472, 2003. © 2003 Wiley-Liss, Inc.

Key words: oligonucleotide analogues; messenger RNA; diagnostic radionuclides; SPECT; PET

*“But I have promises to keep,
And miles to go before I sleep,
And miles to go before I sleep.”*

Robert Frost, “Stopping by the Woods on a Snowy Eve,” 1923.

The elucidation of the rules of Watson–Crick and Hoogsteen base pair formation between nucleic acids ushered in a new promise of the epitome of rational drug design. The basis of this promise was that deleterious genes in disease states could be arrested uniquely at specific DNA or messenger RNA (mRNA) sequences by relatively short complementary oligonucleotides for antigene or antisense therapy, respectively. The concept of using antisense molecules to inhibit gene expression was introduced in 1967 [Belikova et al., 1967], the same year that Khorana published the first method for chemical synthesis of deoxyoligoribonucleotides [Narang et al., 1967]. Ironically, at that time

oligonucleotides no longer than four bases in length could be prepared, and automated solid-phase synthesis of large quantities of longer molecules would not be routine for many years. These challenges have been overcome, and the principles for use of antisense agents in antiviral and cancer therapy are now well defined [Crooke, 1999]. In theory, these same principles could serve as guidelines for the development of labeled antisense oligonucleotide analogues for imaging gene expression in disease states. Yet since 1994, when Dewanjee et al. [1994] produced the first non-invasive tumor image in a living animal model using a radiolabeled antisense oligonucleotide, very few similar studies have been reported in the literature. Real-time, direct, in vivo imaging of endogenous gene expression in animals and humans has still not been demonstrated in a widespread and conclusive manner. This seeming lack of progress may be attributable to various problems antisense imaging agents have exhibited in terms of low target numbers, limited delivery, poor hybridization kinetics and stability, slow clearance, low specificity of localization, high background noise, and several biological barriers to surmount [Blasberg, 2002].

We review here recent developments in antisense imaging technology, which extend the possibility that this modality will soon become an extremely powerful tool for the non-invasive

*Correspondence to: Michael R. Lewis, PhD, Department of Veterinary Medicine and Surgery, College of Veterinary Medicine, 379 E. Campus Drive, University of Missouri-Columbia, Columbia, MO 65211.
E-mail: LewisMic@missouri.edu

Received 9 July 2003; Accepted 10 July 2003

DOI 10.1002/jcb.10641

© 2003 Wiley-Liss, Inc.

study of gene expression *in vivo*. These developments include: (1) new antisense analogues with superior properties for binding macromolecular nucleic acids, (2) advances in radiolabeling chemistry to produce extremely high specific activity antisense imaging agents, (3) novel drug targeting technology to improve *in vivo* specificity, and (4) emerging optical imaging modalities for *in vitro* screening applications and real-time *in vivo* imaging of gene expression. Finally, we will address the crucial issue that antisense imaging must still be proven to result specifically from an *in vivo* antisense mechanism.

ANTISENSE AND MOLECULAR IMAGING

The fundamental processes related to gene expression are now well established. The genetic code carried by DNA is transcribed in the cell nucleus into “blueprints” for protein synthesis in the form of mRNA molecules, which are processed and translocated to ribosomes in the cytoplasm for translation into proteins. Each of these species represents a potential target for molecular imaging of gene expression, and antisense imaging in this context is depicted in Figure 1. A major consideration for *in vivo* imaging relates to the number of target molecules per cell and its effect on generating a sufficient signal-to-noise ratio [Sharma et al., 2002]. Estimates of the number of molecules per

cell for various targets are given in Table I. Most *in vivo* molecular imaging efforts have focused on proteins, such as intracellular receptors, transmembrane receptors, and cell surface or secreted antigens, which are often present in copy numbers ranging from thousands to millions per cell. Such proteins can be detected efficiently using high affinity radioligands for single photon emission computed tomography (SPECT) or positron emission tomography (PET) imaging. In contrast, if DNA is the target, only two molecules per cell could possibly be imaged. Direct imaging of DNA would likely require unprecedented mechanisms of signal amplification to overcome non-specific binding. Moreover, imaging of DNA provides no information on whether a particular gene is actively expressed or contributing to normal versus abnormal cellular function.

Currently, the most widely used strategies for imaging gene expression are termed “direct” and “indirect” approaches [Blasberg, 2002]. Indirect imaging of gene expression often involves a technique called “reporter imaging,” which typically entails the use of an exogenously introduced “reporter gene” and a “reporter probe.” Reporter genes are transcriptionally coupled to the gene of interest and produce proteins that irreversibly trap reporter probes inside transduced cells. Since a large number of reporter probes can accumulate in cells carrying the reporter gene, this strategy has the

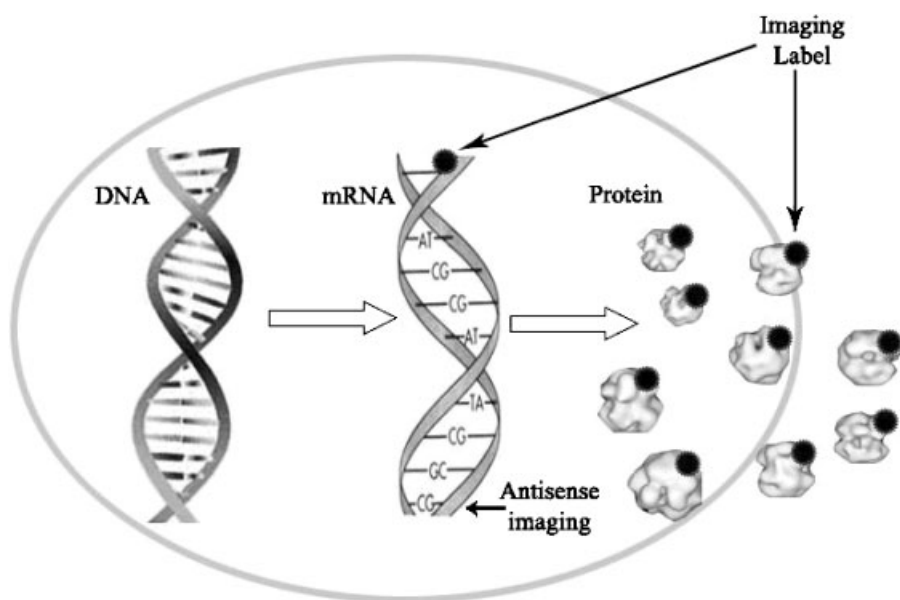


Fig. 1. Schematic representation of antisense imaging in the context of cellular gene expression, contrasted with imaging of proteins and reporter protein function.

TABLE I. Molecular Imaging: Signal Source, Scaling, and Potential Signal-to-Noise Issues*

Signal source	Number of molecules per cell
DNA	2
mRNA	50–1,000s
Protein	100s–1,000,000s
Protein function	Potential for massive signal amplification

*Table courtesy of Dr. David Piwnica-Worms. Adapted from Sharma et al. [2002].

potential for massive signal amplification. However, in this case exogenous protein function is being imaged, as opposed to endogenous mRNA expression.

mRNA is typically present at levels of a few hundred to a few thousand molecules per cell. Unlike DNA, direct imaging of mRNA can provide information on cellular gene expression patterns and may have the potential to detect molecular changes in disease states at relatively early stages, providing opportunities for pre-emptive therapeutic interventions. However, imaging of mRNA based on one-to-one antisense-target interactions still faces considerable challenges, most notably low target numbers and biological delivery barriers. Yet several recent technological advances make it quite possible that true antisense imaging will be realized in the near future.

NEW GENERATION ANTISENSE ANALOGUES

A number of novel oligonucleotide analogues, designed for improved stability, target binding, and antisense activity, have been synthesized and evaluated in vitro and in vivo. The general structures of some of these analogues are shown in Figure 2. As reviewed by Miller [1996], the first antisense agents were unmodified phosphodiester DNAs, but these oligonucleotides are rapidly degraded by nucleases in vivo, greatly limiting their utility for imaging applications. This observation prompted the development of analogues with superior biological stability, such as methylphosphonate derivatives, phosphorothioate DNA, and 2'-*O*-methyl RNA [Miller, 1996]. More recently the ribose scaffold of DNA and RNA analogues has been replaced by a variety of artificial backbones, including peptide nucleic acid (PNA) [Nielsen, 1999], morpholino (MORF) [Summerton and Weller, 1997], and trans-4-hydroxy-L-proline nucleic acid-phosphono nucleic acid (HypNA-pPNA) [Efimov et al., 1999]. Hnatowich and coworkers recently reported preliminary investigations of the newest derivative with potential for antisense imaging: radiolabeled, double-stranded, 2'-*O*-methyl small interfering RNA (siRNA) [Zhang et al., 2003].

DNA phosphorothioates have been investigated most extensively for antisense therapy,

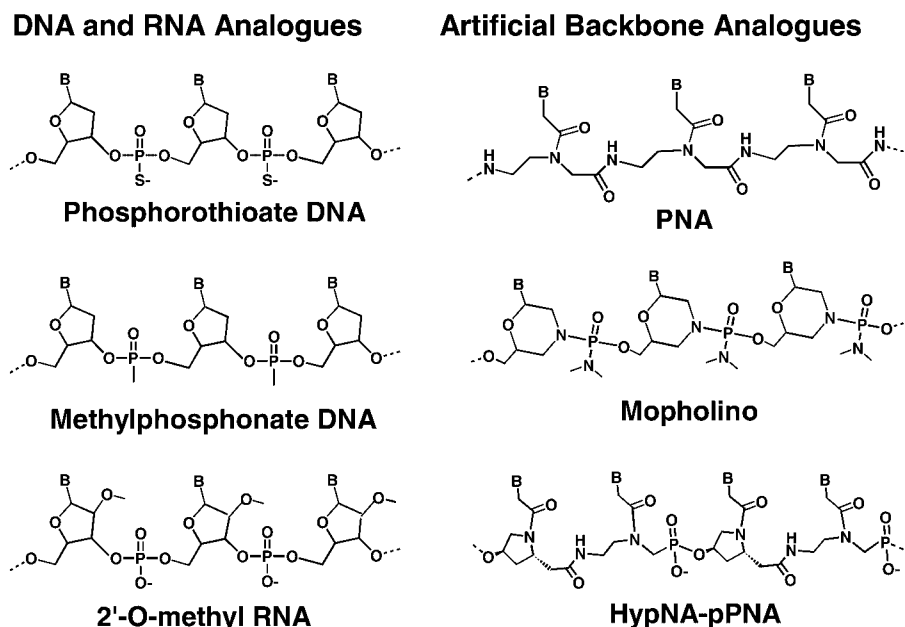


Fig. 2. General structures of some DNA and RNA analogues (**left**) and artificial backbone analogues (**right**) utilized for antisense imaging. B, base.

because of their ability to activate RNase H-mediated degradation of the mRNA target. However, RNase H cleaves DNA:RNA and phosphorothioate DNA:RNA duplexes as short as 5–6 base pairs in length [Summerton, 1999]. This process has significant potential to form transient complexes, leading to the degradation of non-target RNAs and resulting in considerable “non-antisense” effects. Furthermore, phosphorothioate oligonucleotides bind to serum and tissue proteins with high affinity in vivo [Gambhir et al., 1999], resulting in unfavorable pharmacokinetics for imaging. Hnatowich [2000] concluded that RNase H-independent oligonucleotide analogues that do not degrade mRNA may be preferable for antisense imaging. Abrogation of non-specific RNA degradation should afford markedly superior sequence specificity, such that statistically an oligonucleotide of only 13–15 bases is needed to hybridize uniquely to mRNA in the human genome [Summerton, 1999]. Conversely, RNase H activation could result in reduction of the number of target molecules or efflux of the labeled antisense agent, causing loss of target tissue localization [Hnatowich, 2000].

Methylphosphonates, 2'-*O*-methyl RNAs, PNAs, MORFs [Summerton, 1999], HypNA-pPNAs [Efimov et al., 1999], and siRNAs shorter than 19 bases in length [Zhang et al., 2003] are RNase H-independent, thus offering the possibility of superior sequence recognition for antisense imaging applications. However, methylphosphonates exhibit significantly lower affinity binding to complementary RNA than DNA [Miller, 1996], presumably because of steric hindrance by the methyl group. In contrast, 2'-*O*-methyl RNAs [Miller, 1996], PNAs [Nielsen, 1999], MORFs [Summerton and Weller, 1997], and HypNA-pPNAs [Efimov et al., 1999] bind complementary RNA with greater affinity, stability, and mismatch specificity than corresponding DNA:RNA duplexes, potentially rendering them more suitable for antisense imaging.

RADIOLABELING ANTISENSE AGENTS FOR MOLECULAR IMAGING

Physiological steady-state mRNA concentrations typically range from 1 to 1,000 pM [Gambhir et al., 1999; Hnatowich, 2000], and it has been proposed that mRNA concentrations as low as 1 pM can be imaged using antisense

radiopharmaceuticals with specific activities between 1,000 and 10,000 Ci/mmol [Dewanjee et al., 1999]. For in vivo antisense imaging, extremely high specific activity radiolabeling techniques are required to detect low concentrations of target molecules. Antisense deoxyribonucleotides, phosphorothioates, PNAs, and MORFs have been labeled with a variety of radionuclides, including ^{99m}Tc and ^{111}In for SPECT, ^{18}F , ^{11}C , and ^{76}Br for PET, and ^{125}I for autoradiography. The first such radiolabeling method was published by Dewanjee et al. [1991], who labeled a β -actin antisense phosphodiester DNA with ^{125}I at approximately 17 Ci/mmol. Tavitian et al. [1998] developed a general method to label antisense DNA with ^{18}F , ^{76}Br , and ^{125}I , at specific activities as high as 1,000–2,000 Ci/mmol in the case of ^{18}F . Recently, Hnatowich and colleagues have labeled a MORF with ^{111}In at 480 Ci/mmol and ^{99m}Tc at 1,440 Ci/mmol [Liu et al., 2003]. In our group, we labeled an antisense peptide–PNA conjugate targeting the *bcl-2* proto-oncogene with ^{111}In at 1,346 Ci/mmol [Lewis et al., 2002]. The extremely high specific activity radiolabeling methods developed by our group and those of Tavitian and Hnatowich bring in vivo radionuclide imaging of extremely low, physiologically relevant message levels into the realm of possibility.

DRUG TARGETING TECHNOLOGY FOR ANTISENSE IMAGING

“Naked” oligonucleotides, without a drug-targeting carrier, have been employed in most in vivo and clinical studies of conventional antisense therapy. The cellular uptake of phosphodiester and phosphorothioate oligonucleotides is consistent with a low to moderate affinity mechanism of receptor-mediated fluid-phase pinocytosis and adsorptive endocytosis [Summerton, 1999]. However, use of unmodified oligonucleotides without carrier generally results in miniscule accumulation of systemically administered antisense agents in target tissue. This problem has long been recognized in antisense therapy and must be addressed in order to make antisense imaging a useful technique for in vivo molecular detection.

The first carriers developed for intracellular delivery of oligonucleotides were based on technologies utilized for plasmid transfection and gene therapy, including viral vectors,

cationic lipids, and cationic liposomes. Viral vectors are impractical for antisense imaging due to slow and inconvenient formulation, toxicity, and immunogenicity [Hnatowich, 2000]. Cationic lipids and liposomes bind anionic oligonucleotides stably by simple mixing and protect against nuclease degradation [Hnatowich, 2000]. Using PET, Tavitian et al. [2002] found that a new synthetic anionic carrier increased stability, circulation half-life, and organ uptake of a ^{18}F -labeled HIV antisense phosphodiester oligonucleotide in baboons. However, unless modified with molecular targeting vectors, lipid and liposome carriers are likely to have little or no tissue specificity.

Recently, more sophisticated delivery technology has been developed by a number of groups for enhancing tissue targeting and cellular internalization of antisense imaging agents. Much effort has focused on intracellular delivery of antisense PNAs, which exhibit extremely poor cell membrane permeability. This challenge was addressed initially by conjugating antisense PNAs to protein transduction domains (PTDs), like *Drosophila* Antennapedia(43–58) (pAntp) or the HIV Tat peptide. We have coupled our bcl-2 antisense PNA [Lewis et al., 2002] to a synthetic transduction peptide, PTD-4. In cell-free systems, the radiolabeled PTD-4-PNA showed sensitivity and specificity for bcl-2 mRNA equivalent to ^{32}P -labeled bcl-2 antisense DNA, but with superior thermodynamic stability, suggesting that peptide and radiometal chelate conjugation did not compromise target-binding affinity. Another peptide carrier with potential for antisense imaging applications, Pep-1 [Morris et al., 2001], consists of a hydrophobic membrane fusion domain linked to a nuclear localization signal. Pep-1 forms complexes with antisense HypNA-pPNAs and promotes cargo localization to the proper subcellular compartment. A potential drawback of transduction peptides is that they show low cellular specificity. In vivo antisense imaging will likely require vectors with more specific molecular recognition capabilities.

Molecularly targeted drug delivery systems often involve conjugation of antisense imaging agents to high affinity receptor ligands. Mier et al. [2001] conjugated a bcl-2 antisense PNA to tyrosine-3-octreotate, a peptide ligand for tumor-associated somatostatin receptors. The ^{125}I -labeled conjugate displayed high receptor binding affinity and selective in vivo uptake in

CA20948 rat pancreatic tumors. In a similar approach, Thakur and colleagues attached a $^{99\text{m}}\text{Tc}$ -labeled c-erbB-2 antisense PNA to the type 1 insulin growth factor receptor-targeting peptide IGF-1, for in vivo detection of MCF-7 breast cancer xenografts [Rao et al., in press]. Pardridge and coworkers have developed an innovative conjugation of ^{125}I -labeled antisense PNAs to monoclonal antibody OX26 against the rat transferrin receptor [Shi et al., 2000]. Transferrin receptor internalization allowed this conjugate to cross the blood–brain barrier and the brain cell membrane, enabling uptake in brain tumors overexpressing transferrin receptors.

OPTICAL IMAGING OF GENE EXPRESSION

Optical modalities are emerging as powerful tools for imaging exogenous transgene expression in animal models [Ntziachristos et al., 2003]. Development of targeted fluorescent molecular probes, highly sensitive imaging equipment to detect pmol to fmol of probe, and tomographic reconstruction hold great promise for optical molecular imaging in vivo. However, optical imaging of gene expression in humans will require new probes with emissions at near-infrared wavelengths, to provide adequate depth of penetration [Ntziachristos et al., 2003]. Nonetheless, in vitro optical imaging technologies can be applied to screen antisense imaging agents for appropriate cell targeting and subcellular distribution. For example, we have used tetramethylrhodamine-conjugated bcl-2 antisense PNAs and digital scanning confocal fluorescence microscopy to study internalization in Raji lymphoma cells that overexpress the target mRNA [Lewis et al., 2003]. Attachment of *retro-inverso* PTD-4, which has superior proteolytic stability to the native peptide, mediated internalization of the antisense PNA into the cytoplasm, where mRNA concentrations are highest. This finding suggests that the ^{111}In -labeled *retro-inverso* PTD-4-PNA may have some utility for proof-of-principle in vivo imaging.

ANTISENSE IMAGING: IS IT REALLY ANTISENSE?

Only a small number of imaging studies using radiolabeled antisense agents have been published, and some of these do not represent real-time, in vivo antisense imaging. A few PET and

ex vivo autoradiography studies [Tavitian et al., 1998, 2002; Wu et al., 2000] have only examined the pharmacokinetics of antisense oligonucleotides. Kobori et al. [1999] used ex vivo autoradiography to show prominent glioma uptake, in contrast to normal brain tissue, of a ^{11}C -labeled phosphorothioate complementary to glial fibrillary acidic protein mRNA. Pardridge and colleagues have also employed ex vivo autoradiography for antisense detection of brain diseases. In one report, stably transfected, ectopic C6-790 rat gliomas expressing luciferase were visualized using an ^{125}I -antisense PNA-OX26 antibody conjugate [Shi et al., 2000]. In a second publication, an antibody against murine transferrin receptor was conjugated to an ^{125}I -labeled antisense PNA targeting huntingtin mRNA in a transgenic mouse model of Huntington's disease [Lee et al., 2002]. Quantitative autoradiography showed a 3-fold selective sequestration of the antisense radiopharmaceutical in transgenics, compared to littermate controls.

To our knowledge there have been only four published studies of real-time, in vivo antisense imaging in animal models of disease [Dewanjee et al., 1994; Cammilleri et al., 1996; Sato et al., 2001; Rao et al., in press], and a fifth using an artificial animal model designed to demonstrate in vivo antisense hybridization [Mardirossian et al., 1997]. These studies are summarized in Table II. Dewanjee et al. [1994] clearly imaged D1 mouse mammary tumors at 2 h with an intravenously injected ^{111}In -labeled c-myc antisense phosphorothioate oligonucleotide, but not with the ^{111}In -sense probe. Cammilleri et al. [1996] used intratumoral injection of an ^{125}I -phosphodiester complementary to TGF α mRNA to visualize NS2T2A1 human breast tumor xenografts in nude mice. However, no negative controls were performed in that study, and 90% of the radioactivity cleared from the tumor to the intestines and kidneys within 4 h. Kobayashi's group [Sato et al., 2001] administered intraperitoneally an ^{111}In -labeled c-erbB-2 antisense oligodeoxynucleotide, complexed with a polyamidoamine dendrimer or conjugated to avidin, allowing clear detection of intraperitoneal SHIN3 human ovarian tumors in nude mice at 24 h. Again, no negative control experiments were performed. Thakur and colleagues [Rao et al., in press] delineated MCF-7 breast cancer xenografts in mice at 4 h with a $^{99\text{m}}\text{Tc}$ -c-erbB-2 antisense PNA conjugated to

TABLE II. Real-Time, In Vivo Antisense Imaging Studies Reported in the Literature

Analogue ^a	Label	Target	Species, route of administration	Delivery vector	Target tissue uptake ^b	Imaging modality	Reference
PO, PS	^{111}In	c-myc	Tumor-bearing mouse, intravenous	None	Antisense, 11% ID; sense, 1% ID; at 2 h	Planar scintigraphy	[Dewanjee et al., 1994]
PO	^{125}I	TGF α	Tumor-bearing mouse, intratumoral	None	Antisense, 63% ID at 0 h; 6.5% ID at 4 h	Planar scintigraphy	[Cammilleri et al., 1996]
PO	^{111}In	c-erbB-2	Tumor-bearing mouse, intraperitoneal	Dendrimer, avidin	Dendrimer, 9.1% ID/g; avidin, 24% ID/g; at 24 h	Planar scintigraphy	[Sato et al., 2001]
PNA	$^{99\text{m}}\text{Tc}$	c-erbB-2	Tumor-bearing mouse, intravenous	IGF-1R peptide ligand	—	Planar scintigraphy	[Rao et al., in press]
PNA	$^{99\text{m}}\text{Tc}$	"Sense" PNA	Bead-bearing mouse, intravenous	None	"Sense" PNA beads, 0.4% IA/g; uncoupled beads, 0.07% IA/g; at 23 h	Planar scintigraphy	[Mardirossian et al., 1997]

^aPO, phosphodiester; PS, phosphorothioate; PNA, peptide nucleic acid.

^bID, injected dose; IA/g, injected activity per gram of tissue; IA/g, injected activity per gram of tissue.

the IGF-1 receptor ligand. To prove the principle that in vivo antisense hybridization is possible, Hnatowich and coworkers used mice implanted intramuscularly with "sense" PNA coupled to magnetic beads [Mardirossian et al., 1997]. Antisense PNA labeled with ^{99m}Tc showed a 6-fold enhancement of binding to "sense" versus uncoupled beads at 23 h.

Despite preferential accumulation of antisense imaging agents in target tissues, rigorous demonstration of a true in vivo antisense mechanism is still lacking. Since RNase H-independent analogues will likely be used for most future applications, it is our opinion that proof of in vivo antisense targeting will be demonstrated by three phenomena. The first is selective uptake of the antisense agent in tissue stably transfected with the target gene, but not in untransfected tissue. Second, specific target mRNA binding should be demonstrated by RNase protection assays. Thirdly, evidence of target protein synthesis inhibition by Western blotting will show that the mRNA function has been perturbed by a steric translational block.

Some evidence for antisense mechanisms can be gleaned from carefully designed in vitro studies. Using ^{99m}Tc -RI α antisense phosphorothioate in ACHN cells, Hnatowich and coworkers [Zhang et al., 2001] obtained four distinct lines of evidence for an antisense mechanism in vitro. These effects included specific accumulation of approximately 10^5 antisense molecules per cell in ACHN and an additional positive cell line, no specific accumulation in negative cells, increases in total RNA and RI α mRNA synthesis in treated target cells, and a more rapid mass-dependent decrease in antisense versus sense uptake. The accumulation of antisense phosphorothioate was at least two orders of magnitude higher than estimated steady-state mRNA levels, prompting the observation that mRNA turnover/transcription rate may be a more important determinant of antisense accumulation. Our group has obtained similar results with ^{111}In -bcl-2 antisense PNA conjugated to PTD-4 and *retro-inverso* PTD-4 [Jia et al., 2003; Lewis et al., 2003]. These conjugates showed 11-fold increases in uptake over nonsense derivatives in high-bcl-2-expressing Raji cells, as well as 16-fold higher uptake in Raji versus low-bcl-2-expressing U937 cells. Our studies showed selective retention of approximately 2,200 antisense molecules per Raji cell. Compared to phosphorothioates, this lower value may repre-

sent the ability of the transduction peptide to mediate efflux of the PNA conjugate if no retention mechanism comes into play. Pardridge's group showed specific accumulation of ^{125}I -luciferase antisense PNA-OX26 conjugate in transfected versus wild type C6 cells in vitro, but they did not determine if the same phenomenon was observed in vivo [Shi et al., 2000]. However, their antisense targeting of Huntington's disease clearly showed specific in vivo accumulation in transgenic mice compared to controls [Lee et al., 2002]. In that study, specific target mRNA binding was demonstrated by RNase protection and translation arrest assays, but only in cell-free systems, rather than in cell culture or collected tissues.

A major issue yet to be addressed thoroughly for receptor-targeted antisense imaging agents [Shi et al., 2000; Mier et al., 2001; Lee et al., 2002; Rao et al., in press] is that antisense imaging must be distinguished from receptor-mediated uptake. Use of a biologically stable linker between labeled antisense and receptor ligand invokes the question of whether the mRNA or receptor is being imaged. Many receptor-targeting peptides are efficiently trafficked to the lysosome for degradation [Duncan et al., 1997] and may carry the antisense molecule with them. If receptor-avid peptides continue to be used for specific targeting of antisense imaging agents, sophisticated conjugation chemistry may have to be developed to delineate receptor binding from antisense imaging.

In conclusion, it has been over 35 years since the concept of antisense targeting was first introduced and almost 10 years since the first molecular image of a tumor-targeting antisense radiopharmaceutical was produced in an animal model of cancer. Progress in this area has been limited by formidable challenges of surmounting biological barriers to detect low concentrations of target mRNA. However, numerous recent advances in the development of superior antisense molecules, efficient radiolabeling chemistry, sophisticated drug delivery systems, and complementary imaging modalities offer a renewed anticipation that real-time, in vivo antisense imaging will soon be conclusively and widely demonstrated. Perhaps now there are not so many miles to go before we sleep, on the knowledge that antisense technology has become a powerful tool for molecular imaging of endogenous gene expression.

ACKNOWLEDGMENTS

We thank Yongqiang Sui for the preparation of Figure 1, Dr. Geetha Sivaguru, Suzanne Whitmarsh, and Christine Hoeman for assistance in preparing this manuscript, Dr. Mark Hannink for helpful discussions, and Dr. Susan Lever for critically proofreading the manuscript. We also thank the Department of Veterans Affairs, for providing resources and the use of facilities at the Harry S Truman Memorial Veterans' Hospital in Columbia, MO.

REFERENCES

- Belikova AM, Zarytova VF, Grineva NI. 1967. Synthesis of ribonucleosides and diribonucleoside phosphates containing 2-chloroethylamine and nitrogen mustard residues. *Tetrahedron Lett* 37:3557–3562.
- Blasberg R. 2002. Imaging gene expression and endogenous molecular processes: Molecular imaging. *J Cereb Blood Flow Metab* 22:1157–1164.
- Cammilleri S, Sangrajang S, Perdereau B, Brixy F, Calvo F, Bazin H, Magdelenat H. 1996. Biodistribution of iodine-125 tyramine transforming growth factor α antisense oligonucleotide in athymic mice with a human mammary tumour xenograft following intratumoral injection. *Eur J Nucl Med* 23:448–452.
- Crooke ST. 1999. Molecular mechanisms of action of antisense drugs. *Biochim Biophys Acta* 1489:31–44.
- Dewanjee MK, Ghafouripour AK, Werner RK, Serafini AN, Sfakianakis GN. 1991. Development of sensitive radioiodinated anti-sense oligonucleotide probes by conjugation technique. *Bioconjug Chem* 2:195–200.
- Dewanjee MK, Ghafouripour AK, Kapadvanjwala M, Dewanjee S, Serafini AN, Lopez DM, Sfakianakis GN. 1994. Noninvasive imaging of c-myc oncogene messenger RNA with indium-111-antisense probes in a mammary tumor-bearing mouse model. *J Nucl Med* 35:1054–1063.
- Dewanjee MK, Haider N, Narula J. 1999. Imaging with radiolabeled antisense oligonucleotides for the detection of intracellular messenger RNA and cardiovascular disease. *J Nucl Cardiol* 6:345–356.
- Duncan JR, Stephenson MT, Wu HP, Anderson CJ. 1997. Indium-111-diethylenetriaminepentaacetic acid-octreotide is delivered in vivo to pancreatic, tumor cell, renal, and hepatocyte lysosomes. *Cancer Res* 57:659–671.
- Efimov VA, Buryakova AA, Chakhmakhcheva OG. 1999. Synthesis of polyacrylamides N-substituted with PNA-like oligonucleotide mimics for molecular diagnostic applications. *Nucleic Acids Res* 27:4416–4426.
- Gambhir SS, Barrio JR, Herschman HR, Phelps ME. 1999. Imaging gene expression: Principles and assays. *J Nucl Cardiol* 6:219–233.
- Hnatowich DJ. 2000. Antisense imaging: Where are we now? *Cancer Biother Radiopharm* 15:447–457.
- Jia F, Gallazzi F, Shenoy N, Zhang J, Lever SZ, Hannink M, Lewis MR. 2003. Lymphoma cell uptake and retention of radiolabeled bcl-2 antisense peptide-PNA conjugates. *J Nucl Med* 44:370P.
- Kobori N, Imahori Y, Mineura K, Ueda S, Fujii R. 1999. Visualization of mRNA expression in CNS using ^{11}C -labeled phosphorothioate oligodeoxynucleotide. *Neuroreport* 10:2971–2974.
- Lee HJ, Boado RJ, Braasch DA, Corey DR, Pardridge WM. 2002. Imaging gene expression in the brain in vivo in a transgenic mouse model of Huntington's disease with an antisense radiopharmaceutical and drug-targeting technology. *J Nucl Med* 43:948–956.
- Lewis MR, Jia F, Gallazzi F, Wang Y, Zhang J, Shenoy N, Lever SZ, Hannink M. 2002. Radiometal-labeled peptide-PNA conjugates for targeting bcl-2 expression: Preparation, characterization, and in vitro mRNA binding. *Bioconjug Chem* 13:1176–1180.
- Lewis MR, Jia F, Gallazzi F, Landon LA, Shenoy N, Sivaguru G, Hannink M, Lever SZ. 2003. Lymphoma cell uptake of radiometal- and fluorescent-labelled bcl-2 antisense PNA conjugates is mediated by a *retro-inverso* delivery peptide. *J Labelled Cpd Radiopharm* 46:(in press).
- Liu C-b, Liu G-z, Liu N, Zhang Y-m, He J, Rusckowski M, Hnatowich DJ. 2003. Radiolabeling morpholinos with ^{90}Y , ^{111}In , ^{188}Re , and $^{99\text{m}}\text{Tc}$. *Nucl Med Biol* 30:207–214.
- Mardirossian G, Lei K, Rusckowski M, Chang F, Qu T, Egholm M, Hnatowich DJ. 1997. In vivo hybridization of technetium-99m-labeled peptide nucleic acid (PNA). *J Nucl Med* 38:907–913.
- Mier W, Eritja R, Mohammed A, Haberkorn U, Eisenhut M. 2001. Preparation and preclinical development of tumor-targeting peptide-PNA conjugates. *J Nucl Med* 42:115P.
- Miller PS. 1996. Development of antisense and antigene oligonucleotide analogs. In: Cohn WE, Moldave K, editors. *Nucleic acid research and molecular biology*, Vol. 52. San Diego: Academic Press. pp 261–291.
- Morris MC, Depollier J, Mery J, Heitz F, Divita G. 2001. A peptide carrier for the delivery of biologically active proteins into mammalian cells. *Nat Biotechnol* 19:1173–1176.
- Narang SA, Jacobs TM, Khorana HG. 1967. Studies on polynucleotides. LXIII. Deoxyribopolynucleotides containing repeating trinucleotide sequences. The polymerization of protected deoxyribonucleotides. *J Am Chem Soc* 89:2158–2177.
- Nielsen PE. 1999. Applications of peptide nucleic acids. *Curr Opin Biotechnol* 10:71–75.
- Ntziachristos V, Bremer C, Weissleder R. 2003. Fluorescence imaging with near-infrared light: New technological advances that enable in vivo molecular imaging. *Eur Radiol* 13:195–208.
- Rao PS, Tian X, Qin W, Sauter ER, Thakur ML, Wickstrom E. Tc-99m-peptide-PNA probes for imaging oncogene mRNAs in tumors. *Nucl Med Commun* (in press).
- Sato N, Kobayashi H, Saga T, Nakamoto Y, Ishimori T, Togashi K, Fujibayashi Y, Konishi J, Brechbiel MW. 2001. Tumor targeting and imaging of intraperitoneal tumors by use of antisense oligo-DNA complexed with dendrimers and/or avidin in mice. *Clin Cancer Res* 7:3606–3612.
- Sharma V, Luker GD, Pwnica-Worms D. 2002. Molecular imaging of gene expression and protein function in vivo with PET and SPECT. *J Magn Reson Imaging* 16:336–351.
- Shi N, Boado RJ, Pardridge WM. 2000. Antisense imaging of gene expression in the brain in vivo. *Proc Natl Acad Sci USA* 97:14709–14714.
- Summerton J. 1999. Morpholino antisense oligomers: The case for an RNase H-independent structural type. *Biochim Biophys Acta* 1489:141–158.

- Summerton J, Weller D. 1997. Morpholino antisense oligomers: Design, preparation, and properties. *Antisense Nucleic Acid Drug Dev* 7:187–195.
- Tavitian B, Terrazzino S, Kühnast B, Marzabal S, Stettler O, Dollé F, Deverre J-R, Jobert A, Hinnen F, Bendriem B, Crouzel C, Di Giamberardino L. 1998. In vivo imaging of oligonucleotides with positron emission tomography. *Nat Med* 4:467–471.
- Tavitian B, Marzabal S, Boutet V, Kühnast B, Terrazzino S, Moynier M, Dollé F, Deverre JR, Thierry AR. 2002. Characterization of a synthetic anionic vector for oligonucleotide delivery using in vivo whole body dynamic imaging. *Pharm Res* 19:367–376.
- Wu F, Yngve U, Hedberg E, Honda M, Lu L, Eriksson B, Watanabe Y, Bergström M, Långström B. 2000. Distribution of ^{76}Br -labeled antisense oligonucleotides of different length determined ex vivo in rats. *Eur J Pharm Sci* 10:179–186.
- Zhang Y-M, Wang Y, Liu N, Zhu Z-H, Rusckowski M, Hnatowich DJ. 2001. In vitro investigations of tumor targeting with $^{99\text{m}}\text{Tc}$ -labeled antisense DNA. *J Nucl Med* 42:1660–1669.
- Zhang YM, Ding HL, Liu C, He J, Liu N, Xu ZS, Rusckowski M, Hnatowich DJ. 2003. Cell culture studies of double-stranded small interfering RNAs (siRNAs) radiolabeled with $^{99\text{m}}\text{Tc}$. *J Nucl Med* 44:373P–374P.